Assembly and comparative analysis of the complete mitochondrial and chloroplast genome of Cyperus stoloniferus (Cyperaceae), a coastal plant possessing saline-alkali tolerance

Xiaorong Miao
Guangxi University
Wenwen Yang
Guangxi University
Donghai Li
Agricultural College, Yulin Normal University
Aiqin Wang
Guangxi University
Juanyun Li
Agricultural College, Yulin Normal University
Xu Deng
Agricultural College, Yulin Normal University
Longfei He
Guangxi University
Junqi Niu (niujunqi3218@163.com)
Guangxi University

Research Article

Keywords: Cyperus stoloniferus, mtDNA, cpDNA, Comparative analysis, Systematic evolution

Posted Date: February 1st, 2024

DOI: https://doi.org/10.21203/rs.3.rs-3903606/v1

Additional Declarations: No competing interests reported.

Assembly and comparative analysis of the complete mitochondrial and chloroplast genome of *Cyperus stoloniferus* (Cyperaceae), a coastal plant possessing saline-alkali tolerance

Xiaorong Miao[1†], Wenwen Yang[1†], Donghai Li[2], Aiqin Wang[1*], Juanyun Li[2], Xu Deng[2], Longfei He[1], Junqi Niu[1, 2*]

[†]Xiaorong Miao and Wenwen Yang contributed equally to this work.

[*]Correspondence:

Aiqin Wang

Waiqin1966@126.com

Junqi Niu

niujunqi3218@163.com

[1]College of Agriculture, Guangxi University, Nanning 530004, China.

[2]Guangxi Key Laboratory of Agricultural Resources Chemistry and Biotechnology, Agricultural College, Yulin Normal University, Yulin 537000, China.

Full list of author information is available at the end of the article

Abstract

Background *Cyperus stoloniferus* is an important species in coastal ecosystems and possesses economic and ecological value. To elucidate the structural characteristics, variation, and evolution of the organelle genome of *C. stoloniferus*, we sequenced, assembled, and compared its mitochondrial and chloroplast genomes.

Results We assembled the mitochondrial and chloroplast genomes of *C. stoloniferus*. The total length of the mitochondrial genome (mtDNA) was 927,413 bp, with a GC content of 40.59%. It consists of two circular DNA fragments, including 37 protein coding genes (PCGs), 22 tRNAs, and five rRNAs. The length of the chloroplast genome (cpDNA) was 186, 204 bp, containing 93 PCGs, 40 tRNAs, and 8 rRNAs. The mtDNA and cpDNA contained 81 and 129 tandem repeats, respectively, and 346 and 1,170 dispersed repeats, respectively, both of which have 270 simple sequence repeats. The third high-frequency codon (RSCU>1) in the organelle genome tended to end at A or U, whereas that of the low-frequency codon (RSCU<1) tended to end at G or C. The RNA editing sites of the PCGs were relatively few, with only 9 and 23 sites in mtDNA and cpDNA, respectively. A total of 29 mitochondrial plastid DNAs (MTPTs) in the mtDNA were derived from cpDNA, including three complete *trnT-GGU*, *trnH-GUG*, and *trnS-GCU*. Phylogeny and collinearity indicated that the relationship between *C. stoloniferus* and *C. rotundus* is closest. The mitochondrial *rns* gene exhibited the greatest nucleotide variability, whereas the chloroplast gene with the greatest nucleotide variability was *infA*. Chloroplast nucleotide sequences are more conserved than are mitochondrial rRNA gene sequences. Most PCGs in the organellar genome have been

negatively selected and are highly conserved during evolution. Only six mitochondrial genes and two chloroplast genes exhibited Ka/Ks>1, and in particular, *atp9*, *atp6*, and *rps7* may have undergone potential positive selection.

Conclusion We assembled and validated *C. stoloniferus* mtDNA, that contained a 15,034 bp reverse complementary sequence. The organelle genome sequence of *C. stoloniferus* provides valuable genomic resources for species identification, evolution, and comparative genomic research in Cyperaceae.

Keywords *Cyperus stoloniferus*, mtDNA, cpDNA, Comparative analysis, Systematic evolution

Background

Cyperus stoloniferus Retz., a perennial herbaceous plant of the Cyperaceae family (sedges), primarily grows on coastal sand dunes or beaches. It is predominantly in the coastal areas of China, Japan, and Southeast Asia (https://www.gbif.org/species/2714571). *C. stoloniferus* exhibits thick and narrow rhizomes, creeping and interlocking growth, and high population density and is an important sand-fixing plant along the coastline [1]. *C. stoloniferus* is also a precious species in coastal ecosystems with potential economic and ecological value and has been included in the Germplasm Resources of Halophytes in China (http://www.grhc.sdnu.edu.cn/info/1008/1374.htm). *C. stoloniferus* is an important medicinal plant used to treat menstrual disorders, dysmenorrhea, stomach pain, and inflammation [2, 3], and it was included in the IUCN Red List of Threatened Species in 2010. Due to its wide distribution and lack of threat to survival, it is one of the species

of least concern [4]. Currently, relatively little research has been conducted examining *C. stoloniferus*, and this greatly limits our understanding of its evolutionary characteristics and utilization.

Cyperaceae is the third largest monocotyledonous plant family with over 5,500 species. Based on morphological characteristics such as flowers, inflorescences, spikelets, and embryos, they can be divided into 90 genera and play key roles in wetland and alpine ecosystems [5, 6]. In recent years, based on partial nuclear DNA and plastid genes (*matK*, *rbcL*, *rps*16, etc), studies have determined that certain species with similar morphologies may belong to different genera, whereas species with significant morphological differences may belong to the same genus. This has caused confusion in regard to species identification and sparked controversy in the taxonomy of Cyperaceae [7–9]. Therefore, more comprehensive explorations should be conducted such as HybSeq bait and targeted sequencing combined with traditional classification, to establish more accurate and reliable classification systems [10, 11].

Cyperaceae species possess adaptive characteristics such as C4 photosynthesis, dispersed centromeres, and multiple origins of holocentric chromosomes, thus making it an ideal group for studying evolutionary biology [8, 12, 13]. Plants possess three relatively independent genomes, including the nuclear genome, chloroplast genome (Chloroplast DNA, cpDNA), and mitochondrial genome (mitochondrial DNA, mtDNA). The chloroplast and mitochondrial genomest are often referred to as organelle genomes. As of January 26, 2024, the nuclear genomes of only 11 species of Cyperaceae have been reported, including seven genera of *Carex*, three genera of

Rhynchospora, and one genus of *Cyperus* (https://www.plabipd.de/plant_genomes_pa.ep). In the NCBI database, there are over 40 complete cpDNAs of plants in the family Cyperaceae, whereas mtDNAs have only been published for *C. rotundus*, *C. esculentus* [14], and *Carex breviculimis* [15]. Compared to the nuclear genome, plant organelle genomes are highly conserved and evolve rapidly, and they exhibit maternal inheritance. They provide an ideal tool for tracing species origin, phylogeny, and molecular ecology[16–18]. Due to the lack of genomic data, Cyperaceae has not yet been systematically classified based on the complete organelle genome, thus leading to uncertainty regarding the evolutionary relationships of *C. stoloniferus*.

Therefore, we used next-generation sequencing (NGS) and third-generation sequencing (TGS) to assemble the organellar genome of *C. stoloniferus*. The structural characteristics, gene composition, repeat sequences, codon preferences, RNA editing, and sequence transfer of the mitochondrial and chloroplast genomes were compared and analyzed along with genomic collinearity, gene nucleotide diversity, and selection pressure of related species. A phylogenetic tree was constructed using the shared mitochondrial and chloroplast genes, thus providing valuable genomic resources for the classification, population genetics, and evolution of *C. stoloniferus*.

Results

Assembly validation, structural characteristics and gene composition of organelle genomes in *C. stoloniferus*

Based on the sequencing data, we spliced and assembled mtDNA and cpDNA from *C.*

stoloniferus. Visualization results using Bandage software [19] demonstrated that the mtDNA possessed two discrete DNA fragments termed mtDNA 1 (mt1) and mtDNA 2 (mt2), respectively, without overlapping nucleotide sequence regions (Fig. 1A). However, mt2 consisted of three overlapping contig1, contig2, and contig3 regions with lengths of 531,572, 15,034, and 84,963 bp, respectively. Based on this observation, we propose the primary cyclic structure of contig1+contig2 (+) +contig3+contig2 (-) for mt2, where contig2 is a reverse complementary sequence (Fig. 1B). To confirm the contig splicing hypothesis, we designed four pairs of PCR primers for PCR amplification and Sanger sequencing of four overlapping regions (P1, P2, P3, and P4). The four contig binding sites of mt2, PCR primers, and PCR conditions are listed in Table S1. The 1% agarose gel electrophoresis band of the PCR amplification product was consistent with the expected sequence size (Fig. 1C), and Sanger sequencing results confirmed the correctness of this contig combination (Fig. S1). Additionally, PCR amplification did not detect the target gene sequences of P5, P6, P7, and P8, thus indicating that contig1 and contig2, and contig3 and contig2 cannot form circular DNA alone (Fig. 1D). The above results demonstrate that mt2 exhibits only one conformation, that is the primary circular DNA composed of contig1, contig2 (+), contig3, and contig2 (-).

The lengths of mt1 and mt2 were 280,810 and 646,603 bp, respectively, with a GC content of 40.59% (Fig. 2 and Table 1). A total of 37 protein coding genes (PCGs) (mt1:9 and mt2:28), 22 tRNAs (mt1:12 and mt2:10), and 5 rRNAs (mt1:2 and mt2:3) were annotated in the mtDNA of *C. stoloniferus*. *TrnE-TTC*, *trnK-TTT*, *trnM-CAT*, and

a*tp8* each possessed two copies and lacked tRNAs for transporting alanine (A), valine (V), leucine (L), and threonine (T) (Table 2).

The length of the cpDNA of *C. stoloniferus* was 186,204 bp, and the GC content was 33.19%. It possesses a typical tetrad circular structure with two reverse repeat sequence regions (IRs), a large single-copy region (LSC), and a small single-copy region (SSC) with lengths of 74,842 (GC, 37.33%), 101,039 (GC, 30.93%), and 10,323 bp (GC, 25.13%), respectively. A total of 141 genes were annotated, including 93 PCGs, 8 rRNAs, and 40 tRNAs (Table S2). Among these genes, 24 genes possessed two copies, *rpl32* and *trnH-GUG* possessed three copies, and *trnfM-CAU* possessed four copies. The total lengths of the mtDNA and cpDNA coding sequences were 42,632 and 79,714 bp, respectively, and accounted for 4.60% and 42.81% of their genomes. Non-coding sequences accounted 95.04% and 57.09%, respectively (Table S3). This was very similar to the proportion of non-coding sequences in the mtDNA of *C. esculentus* (95.36%) [14].

A total of 23 genes in the organelle genome of *C. esculentus* possessed introns, and of these, 18 genes possessed one intron, *ycf3* possessed two, and *nad4* possessed four. Simultaneously, trans-splicing was observed in *nad1*, *nad2*, *nad5*, and *rps12* (Table S4). The two exons of trans-splicing are derived from different pre-mRNAs, and evidence of trans-splicing introns in these genes has been observed in *Nymphaea* plants [20].

Organelle genome repeat sequences

Repetitive sequences not only play an important role in maintaining the advanced structure of the genome, but also play a crucial role in driving evolution, inducing

158 variations, and regulating gene expression [21, 22]. Therefore, we analyzed the
159 dispersed repeats, microsatellites, and tandem repeats of the *C. stoloniferus* organelle
160 genomes (Fig. 3A). Microsatellites, also known as simple sequence repeats (SSRs), are
161 DNA fragments composed of short sequence repeat units with a length of 1-6 base pairs
162 that are distributed throughout the entire genome [23]. In the present study, 270, 77,
163 and 193 SSRs were detected in cpDNA, mt1, and mt2, respectively (Fig. 3B). The SSRs
164 of mtDNA and cpDNA were primarily tetranucleotide repeats with the lowest number
165 of hexanucleotide repeats. There were 29, 64, and 93 tetranucleotide repeats in mt1,
166 mt2, and cpDNA, respectively, accounting for 37.66%, 33.16%, and 48.19% of the total
167 number of SSRs in the genome (Tables S5-S7).

168 Totals of 25, 56, and 129 tandem repeats were identified in mt1, mt2, and cpDNA,
169 respectively (Fig. 3C, Tables S8-S10). The cpDNA detected 1,170 dispersed repeats,
170 including 777 forward repeats, 376 reverse repeats, 7 complementary repeats, and 10
171 palindromic repeats. mt1 and mt2 contained 66 and 280 dispersed repeats, respectively.
172 Among them, mt1 did not possess complementary repeats, while mt2 did not possess
173 complementary and reverse repeates (Fig. 3C, Tables S11-S13). These dispersed repeats
174 ranged from 30 to 15,034 bp in length. The total lengths of cpDNA, mt1, and mt2
175 dispersed repeat sequences were 105,087, 2,622, and 28,346 bp, respectively,
176 accounting for 56.44%, 0.93%, and 4.38% of the genome, respectively. These rich
177 repetitive sequences provide important data for screening of molecular markers for
178 studying the genetic diversity of *C. stoloniferus*.

179 **Gene codon preference**

Codon preference refers to the difference in the frequency of use of degenerate codons by organisms during the translation process and the formation of a set of commonly used codons that are adapted to it during evolution, and this is of great significance for gene expression [24]. Codon preference can be represented by Relative synonymous codon usage (RSCU), with RSCU values ranged from 0 to 2, where RSCU = 1 represents the expected usage frequency, RSCU < 1 indicates that the codon usage frequency is lower than the expected value, and RSCU > 1 indicates that the codon usage frequency is higher than the expected value [25]. At RSCU>1, mt1, mt2, and cpDNA contained 26, 28, and 31 codons, respectively (Fig. 4), thus indicating that the organelle genes of *C. stoloniferus* preferred to use these codons. Among these high-frequency codons (RSCU>1), the third codon position was A or U, and accounted for 94.63% and 97.35% of the mitochondrial and chloroplast codons, respectively. In low-frequency codons (RSCU<1), the third codon position was G or C, and accounted for 76.86% and 93.41% of mitochondrial and chloroplast codons, respectively. This is a common characteristic of codon bias in terrestrial plant organelle genomes [26].

The most frequently used synonymous codons for mt1, mt2, and cpDNA in *C. stoloniferus* were UGA (Ter: RSCU=1.71), UAA (Ter: RSCU=2.05), and UUA (Leu: RSCU=2.27), respectively. The least frequently used synonymous codons were UAG (Ter: RSCU=0.43), UAG (Ter: RSCU=0.27), and CUG (Leu: RSCU=0.24), with only AUG (Met) exhibiting RSCU=1 (Table S14). The most frequently used codons for mtDNA and cpDNA were UUU and AUU with 445 and 815 codons, respectively. The termination codon of mt1 tended to be UGA, whereas mt2 and cpDNA tended to be

UAA. The total codon-related parameters of the organelle genome, including ENC, CAI, GC1, GC2, GC3, T3s, C3s, A3s, and G3s, are detailed in Table S15.

RNA editing

RNA editing is the phenomenon of base insertion, deletion, or alteration that occurs during DNA transcription to form RNA, and this exists in the mitochondria, chloroplasts, and nuclei [27]. By mapping transcriptome data to mtDNA and cpDNA, nine and 23 RNAediting sites were identified in the mitochondrial and chloroplast genes of *C. stoloniferus*, respectively (Fig. 5). Six genes were detected in mtDNA that may have undergone RNA editing, including *ccmC*, *matR*, *mttB*, *nad7*, *rpl16*, and *rps19*, but they were not detected in mt1. There are eight genes in cpDNA that include *atpB*, *atpF*, *petA*, *psbL*, *psbT*, *rpoA*, *rpoB*, and *rpoC2*. Eight codons were converted to leucine, and accounted for 27% of the RNA editing sites, thus indicating the highest tendency for RNA editing to convert to leucine. In the mitochondria and chloroplasts, 88.89% and 78.26%, respectively, were identified above the first two bases of the codon, thereby altering the corresponding amino acids (Table S16). All mitochondrial RNA editing sites were C-U-edited, whereas chloroplast C-U-edited sites accounted for only 30.43%. RNA editing may form termination codons, ultimately leading to the premature termination of chloroplast *atpF*, *psbT*, and *rpoC2* translation. After RNA editing, 55.56% of the hydrophilic amino acids in the mitochondria were converted into hydrophobic amino acids compared to only 13.04% in the chloroplasts. Meanwhile, 30.43% of the hydrophilic amino acids in the chloroplasts were converted into other hydrophilic amino acids, but this did not occur in the mitochondria (Table S17).

Plastid DNA transfer

mtDNA generally contains sequences derived from plastid DNA, known as mitochondrial plastid DNA (MTPT) [28]. Based on nucleotide sequence similarity, 29 MTPTs were identified in the mtDNA of *C. stoloniferus* that possibly originated from cpDNA, with lengths ranged from 53 to 1,831 bp (Fig. 6). The total lengths of the MTPTs was 8,710 bp, accounted for 4.68% of the cpDNA. Among these MTPTs, 19 were chloroplast genes (most of which were gene fragments) such as *accD*, *atpA*, *ndhA*, *ndhH*, *rpoC1*, *rps12*, *rps15*, *rrn16*, and *rrn23*. Among these, there were only three complete genes that included *trnT-GGU*, *trnH-GUG*, and *trnS-GCU* (Table S18).

mt1 and mt2 possessed nine and 20 MTPTs, respectively, with a total length of 10,186 bp, that accounted for 1.1% of the mtDNA. Surprisingly, chloroplast *trnT-GGU* was transferred to mtDNA and transformed into *trnM-CAT*, thus indicating that base mutations may occur during sequence transfer. Additionally, some small fragment sequences derived from chloroplasts were subsets of larger fragment sequences or appeared multiple times in mtDNA, thus indicating that these fragments may have undergone multiple independent transfer integrations, replications, and recombinations within the mtDNA after transfer integration [29].

Phylogenetic analysis

To identify the phylogenetic status of *C. stoloniferus*, *Toona ciliata* and *T. sinensis* of Meliaceae were used as outgroups. Based on the shared genes of the mitochondria and chloroplasts, we used the maximum likelihood (ML) method to analyze the evolutionary relationships of nine closely related species. A phylogenetic tree

constructed from the 27 mitochondrial PCGs shared by the 11 plant species is presented in Fig. 7A. The results indicated that in Cyperaceae, the closest relative to *C. stoloniferus* was *C. rotundus*, and this was followed by *C. esculentus*. The farthest was *C. brevicullis*. The phylogenetic tree constructed from the 68 chloroplast PCGs (Fig. 7B) also indicated that the overall structures of the two phylogenetic trees were the same, thus further confirming the evolutionary relationship of these four sedge plants.

The phylogeny also indicated that Cyperaceae was closely related to Juncaceae, whereas Poaceae was more distant. Further research determined that mitochondria in Juncaceae possess *rps10* and *rps14* that are missing in Cyperaceae and Poaceae (Table S19). In Cyperaceae and Juncaceae, chloroplasts lacked *clpP* and *ycf15*, whereas in Cyperaceae, *rpl23* was missing, but there were two *ycf68* (Table S20). The occurrence of loss, addition, and replication events of organelle-functional genes in the same family is consistent with the results of phylogenetic clustering [30].

Collinearity of organelle genome in Cyperaceae

Analysis of regions collinear with organelle genomes in the four sedge plants revealed numerous homologous collinear fragments (Fig. 8). There were 62, 60, and 47 collinearity blocks with mtDNA lengths of greater than 5,000 bp between *C. stoloniferus* and *C. rotundus*, *C. stoloniferus* and *C. esculentus*, *C. esculentus* and *C. breviculis*, respectively (Table S21). There were eight, 14, and six collinearity blocks with cpDNA lengths of greater than 5,000 bp between *C. stoloniferus* and *C. rotundus*, *C. stoloniferus* and *C. esculentus*, *C. esculentus* and *C. breviculis*, respectively. However, the eight collinear blocks between *C. stoloniferus* and *C. rotundus* were >

10,000 bp long, whereas the blocks between *C. esculentus* and *C. breviculis* were less than 10,000 bp long (Table S22). Additionally, *C. stoloniferus* and *C. rotundus* were the longest among all collinearity blocks, with 53,854 and 47,814 bp, respectively, thus indicating that the closer the species relationship, the longer the collinearity block.

Meanwhile, there were differences in the collinear block arrangement positions of mtDNA (or cpDNA) in Cyperaceae, indicating that compared to closely related species, the organellar genome of *C. stoloniferus* undergoes extensive genomic rearrangement. Additionally, certain regions of mtDNA and cpDNA in *C. stoloniferus* do not share homology with those of other species, thus indicating that they exist only in the organellar genome of *C. stoloniferus*.

Nucleotide diversity

Nucleotide diversity (Pi) can be used to evaluate genetic differences in nucleotide sequences between different species and populations, and regions with high variability can be selected as potential molecular markers for populations [31]. Pi analysis of organelle genes was conducted on nine closely related plants, and the results indicated that the mitochondrial gene with the highest variability was *rns* (Pi=0.23425). This was followed by *atp8* (Pi=0.1664) and *mttB* (Pi=0) (Fig. 9A). In the mitochondrial PCGs, only five genes exhibited Pi>0.10, whereas the remaining 26 genes possessed Pi values ranging from 0 to 0.07535, thus indicating that the nucleotide sequences of most genes in the mitochondria of *C. stoloniferus* were highly conserved.

The Pi values of chloroplast PCGs ranged from 0 to 0.24609, with 51 genes less than 0.10 (Fig. 9B, 9C, and Table S23). Among them, *infA* (Pi=0.24609) exhibited the

greatest variability, and this was followed by *rps18* (Pi=0.2028), *rpl22* (Pi=0.18676), and *rpoA* (Pi=0.18614) that also exhibited greater variability. In contrast, the most conserved genes were *accD* (Pi=0.00293) and *ycf2* (Pi=0). Additionally, the Pi values of the four chloroplast rRNA genes were less than 0.05, whereas the Pi values of the three mitochondrial rRNA genes were greater than 0.108, thus indicating that the nucleotide sequence of the chloroplast rRNA gene in *C. stoloniferus* was more conserved than that of the mitochondria.

Ka/Ks analysis of PCGs

Ka/Ks (also known as dN/dS) represents the ratio of the nonsynonymous substitution rate (Ka) to the synonymous substitution rate (Ks) that is used to measure the protein selection pressure in the evolutionary process of different species [32]. When Ka/Ks>1, genes undergo positive selection. When Ka/Ks=1, the gene undergoes neutral evolution. When Ka/Ks<1, genes are subjected to negative or purifying selection [33]. To evaluate the selection pressure on PCGs in closely related plants of *C. stoloniferus*, we calculated the Ka/Ks of 27 mitochondrial and 68 chloroplast genes. The results are presented in Fig. 10A, where 21 mitochondrial PCGs exhibited Ka/Ks <1, particularly *atp1* (Ka/Ks=0.0746) and *cox1* (Ka/Ks=0.07223) (Table S24), thus indicating that these genes have undergone purification selection and have relatively stable protein functions. In contrast, the average Ka/Ks values of *atp6*, *atp9*, *ccmC*, *ccmFN*, *rpl16*, and *rps3* were >1, and *atp9* (Ka/Ks=2.15) and *atp6* (Ka/Ks=1.61) were strongly and positively selected. Compared to mitochondrial genes, the average Ka/Ks values of *rps7* and *rrn16* in chloroplasts were greater than 1, whereas the Ka/Ks values of the remaining 66 genes

were less than 1 (Fig. 10B and 10C), thus indicating that most PCGs in chloroplasts exhibited negative selection and were highly conserved during evolution.

Discussion

Structural characteristics of plant organelle genome

In recent years, with the rapid development of sequencing and assembly technologies the number of high-quality organellar genome assemblies has rapidly increased. Currently, 6,804 cpDNA and 433 mtDNA sequences have been sequenced from plants [34]. The structure and genetic composition of cpDNA are highly conserved. however, due to their relatively unique genetic background and evolutionary history, there are differences in the size of cpDNA among different species, where they generally range in length from 107 to 218 kb [35]. cpDNA sizes of the *C. stoloniferus*, *C. rotundus* [36] and *C .esculentus* [37] in the genus *Cyperus* are approximately 186 kb, and their GC content is extremely similar, and range from 33.19% to 33.26%.

Compared to cpDNA, plant mtDNA is generally larger and more complex, with not only single circular DNA, polycyclic DNA [38], and linear DNA [39], but also possibly complex structure DNA [40, 41]. Species such as *Camellia sinensis* [42], *Coptis deltoidei* [43], *Fallopia multiflora* [44], and *Prunella vulgaris* [45] possess two circular DNA in their mtDNA, while buckwheat possesses 10 [46] and *Amorphophallus albus* possesses 19 [47]. This study also confirmed that the mtDNA of *C. stoloniferus* possesses two circular DNA, whereas *C. esculentus* with a closer genetic relationship possesses only one [14], and *C. breviculmis* with a further genetic relationship may exhibit four different conformations [15]. Most plant mtDNAs exhibit a circular

structure containing the entire genome sequence, and some homologous sequences may undergo recombination, ultimately resulting in the formation of small circular structures. Small circular DNA, linear DNA, and primary circular DNA may coexist in plant mtDNA [39].

Genomic evolution

Most higher plants exhibit little or no homologous recombination in their cpDNA, and their gene composition and nucleotide sequence are conserved [48]. However, mtDNA also exhibits a highly conserved and different evolutionary rate compared to that of nuclear genes, and this can provide a large amount of classification information and can be used for the classification and identification of closely related species [49, 50]. The spikelets of Poaceae and Cyperaceae were similar. Chromosomes and pollen morphology indicate a close relationship between Cyperaceae and Juncaceae, while phylogenetic analysis suggests that Cyperaceae possesses a closer genetic relationship with Juncaceae and a farther relationship with Poaceae [51, 52]. This study also demonstrated this evolutionary relationship by constructing a phylogenetic tree based on shared genes between mitochondria and chloroplasts.

C. rotundius and *C. esculentus* began to differentiate approximately 5.6 million years ago, although they share very similar morphological characteristics, growth habits, habitats, and growth and development processes [53]. However, the results of systematic evolution indicated that the phylogenetic relationship between *C. rotundius* and *C. stoloniferus* was the closest, and this was followed by *C. esculentus*. This study is the first to elucidate the evolutionary relationships among these three sedge species.

The maximum collinear region of mtDNA in Cyperaceae is approximately 53.85 kb, whereas the maximum collinear region of cpDNA is approximately 47.81 kb. Collinear regions were observed in both *C. stoloniferus* and *C. rotundius*, thus further indicating their close genetic relationship. However, species with distant genetic relationships also possess smaller collinear blocks, and this may be due to the highly dynamic structure of plant organelle genomes that are still evolving [34].

A large number of tandem repeats, dispersed repeats, and SSRs were detected in both the mtDNA and cpDNA of *C. stoloniferus*. Concurrently, it was observed that genes such as *rns*, *atp8*, *infA*, *rps18*, *rpl22*, and *rpoA* exhibited high Pi values. These are not only important sources of information for developing populations and evolutionary analysis markers but also play an important role in genome plasticity and adaptive evolution [54]. Additionally, certain noncoding regions of cpDNA exhibit relatively high nucleotide substitution rates that are not only suitable for reconstructing phylogenetic relationships between species but also for studying phylogenetic geography within species [55, 56]. Therefore, the organellar genome contributes to genetic diversity, and lineage geography research focused on *C. stoloniferus* helps to trace the historical origins of existing distribution patterns and elucidates the impact of geological changes on the evolution of *C. stoloniferus*.

Genomic sequence transfer

During plant evolution, mtDNA has undergone significant changes in its gene sequence, genome structure, and sequence transfer from other organelles [57]. Plasmid DNA fragments are commonly transferred to mtDNA, and this frequent DNA transfer can be

traced back to the common ancestor of gymnosperms and angiosperms approximately 300 MYA [28]. As evolution progresses, cpDNA gradually decreases, whereas mtDNA gradually expands due to frequent DNA exchange with the nucleus and chloroplast genome [58]. This study also determined that the mtDNA of *C. stoloniferus* is 9.27 Mb, and this is 4.98-fold larger than that of cpDNA. Plasmid transfer DNA fragments are randomly dispersed in cpDNA, with a total length of 3.19 kp in *C. esculentus* [37], 5.67 kp in *C. breviculimis* [15], and 8.71 kp in *C. stoloniferus*. It is currently the longest known plant plasmid in the family Cyperaceae and transfers plastid DNA to mtDNA.

Horizontal gene transfer (HGT) has been proposed relative to vertical gene transfer (parental transfer to offspring), and this overcomes the limitations of genetic relationships and makes gene flow more complex [59]. Due to the lack of data regarding the nuclear genome of *C. stoloniferus*, further research is required to determine if DNA transfer occurs between the nuclear genome and the mitochondrial and chloroplast genomes.

RNA editing

Plant organelle gene expression involves many different co-transcriptional or post transcriptional nucleic acid modifications, including 5'and 3' RNA processing, cis- and trans-splicing, and RNA editing [27]. RNA editing involves the production of RNA products that differ from the DNA templates and can alter genetic information at the mRNA level. The transformation of C to U in plant mtDNA and cpDNA is the primary type of RNA editing [60]. The mitochondrial genes of *C. stoloniferus* belonged to the C-U editing type, whereas the chloroplast genes accounted for 30.43% of the total. RNA

editing not only leads to changes in the encoded amino acids but may also generate termination codons, ultimately leading to premature termination of the translation process [61]. In the organelle genome of *C. stoloniferus*, this phenomenon may occur in *atpF*, *psbT*, and *rpoC2*.

The number of RNA editing sites in organellar genomes varies among species, with many gains and losses at editing sites [62]. In terrestrial plants, the number of RNA-editing sites ranges from zero to several hundred. The number of editing sites decreases with plant evolution, and editing events occur more frequently in early differentiated plants than they do in late-differentiated plants, thus indicating that RNA editing may occur simultaneously in early differentiated plants of different branches and incur significant losses during the evolutionary process [63]. The loss of a large number of RNA-editing sites in the organelle genome of *Welwitschia mirabilis* cells may also be caused by reverse transcription processing, and a few retained editing sites may also exist in genes with lower expression levels [64]. This study also observed that the organelles of *C. stoloniferus* possess fewer editing sites, and this could be important for future research examining RNA editing in Cyperaceae.

Gene selection pressure

A long-standing issue in evolutionary biology is how natural selection and environmental pressures shape plant genome structures. The Ka/Ks of most genes in the organelle genome of *C. stoloniferus* were less than 1, as nonsynonymous substitutions generally produce harmful traits, and only in a few cases can they lead to evolutionary advantages. This is consistent with previous research results [33, 65]. This

study determined that the Ka/Ks values of *atp6*, *atp9*, and *rps7* were >1, thus indicating that these genes have undergone positive selection and are rapidly evolving, and this may be related to the adaptation of *C. stoloniferus* to coastal environments. Mitochondria are the primary sites for generating the energy required for cellular activity in plants. *atp6* and *atp9* are located on the inner mitochondrial membrane and are important components of the ATP synthase complex [66]. They are potential drivers of mtDNA evolution and are often used in CMS breeding [55, 67]. Similar to the growth environment of *C. stoloniferus*, it has been observed in mangroves that only the *rps7* gene is positively selected [68]. However, whether these genes were selected under environmental stress to produce new functions for adaptation to coastal environments requires further investigation.

Conclusion

In this study using the Illumina and Nanopore sequencing platforms, we assembled for the first time the mitochondrial and chloroplast genomes of *C. stoloniferus*, and this is also the fourth complete mtDNA of Cyperaceae. PCR amplification and Sanger sequencing confirmed that the mtDNA of *C. stoloniferus* possessed two circular DNAs, among which mt2 possessed a 15,034 bp reverse complementary sequence, thus confirming the authenticity of the complex genome structure of Cyperaceae. Furthermore, a comparative analysis was conducted to examine the gene composition, repeat sequences, codon preference, RNA editing, and nucleotide diversity of the organellar genome of *C. stoloniferus*. A total of 29 MTPTs were observed to originate from cpDNA with a length of 10,186 bp and accounting for 1.1% of the mtDNA,

including three complete *trnT-GGU*, *trnH-GUG*, and *trnS-GCU*. The selection pressure results indicated that mitochondrial *atp6*, *atp9*, *ccmC*, *ccmFN*, *rpl16*, and *rps3* and chloroplast *rps7* and *rrn16* have undergone potential positive selection, thus revealing that these genes may play a role in the adaptation of *C. stoloniferus* to coastal environments. Genomic evolution and collinearity analyses indicated that the genetic relationship between *C. stoloniferus* and *C. rotundius* is the closest. These results will help researchers understand the characteristics of organelle genomes in Cyperaceae and lay the foundation for further elucidation of the evolutionary relationships of Cyperaceae.

Methods

Plant materials and genome sequencing

C. stoloniferus was collected from the coast of Jiangshan Town, Fangchenggang City, Guangxi Province, China (108° 33'E and 21° 68'N), by Li Donghai and identified by Professor Wang Aiqin from Guangxi University. It is currently stored in the characteristic plant herbarium of Southeast Guangxi, Yulin Normal University, under plant specimen number LM202118. Using young leaves of *C. stoloniferus*, an improved CTAB method was utilized to extract total DNA [69]. NanoDrop and agarose gel electrophoresis were used to assess DNA purity, concentration, and integrity. A Nextera XT DNA library preparation kit (Illumina Inc., San Diego, CA, USA) was used to construct a cDNA sequencing library with an average length of 350 bp. Quality control was performed on the sequencing data using the Illumina NovaSeq 6000 platform for high-throughput sequencing, and low-quality sequences were removed to obtain 11.45

Gb of clean sequencing data. Using the SQK-LSK109 linker kit to construct a cDNA library, high-throughput sequencing was performed using Oxford nanopore technologies, ultimately resulting in clean sequencing data of 12.73 Gb with an average length of 9,342 bp, N50 of 12,345 bp, and N90 of 6,072 bp (Table S25).

Genomic assembly and annotation

We separated mitochondrial and chloroplast DNA sequences from the sequencing data and edited the original read length using the NGS QC Tool Kit v2.3.3 software [70]. Using the mitochondrial and chloroplast genomes of *C. esculentus* as a reference, the reads were iteratively extended and spliced using the PRIME software [71] and SPAdes 3.11.0 software [72]. The Mitofey software（http://dogma.ccbb.utexas.edu/mitofy）was used for gene annotation. After annotation, Se-quin files were output, manually corrected, and submitted to the NCBI database.

Identification of repetitive sequences

SSRs were detected using online MISA software (https://webblast.ipk-gatersleben.de/misa), with parameter settings following Xia's method [41]. Tandem repeat sequences were identified using the online Tandem Repeat Finder software (https://tandem.bu.edu/trf） with default parameters [73]. Using online Repeater software (https://bibiserv.cebitec.uni-bielefeld.de/reputer) for dispersed repeats identification, the parameter settings refer to Xia's method [41] for analyzing the number of forward repeats, reverse repeats, complementary repeats, and palindrome repeats.

Identification of codon preference

To increase the accuracy of the data, only genes with a length of ≥ 300 bp were analyzed. Using the Perl script, 7, 22, and 51 PCGs were screened from mt1, mt2, and cpDNA, respectively. CodonW v1.4.2 software (https://sourceforge.net/projects/codonw) was used to analyze the RSCU, T3s, C3s, A3s, G3s, CAI, CBI, and ENC of the PCGs codons. Online Cusp software (http://emboss.toulouse.inra.fr/cgi-bin/emboss/cusp) was used to analyze the GC content of the first, second, and third codons (GC1, GC2, and GC3, respectively).

Identification of RNA editing

The TopHat2 software was used to map the raw transcriptome data of *C. stoloniferus* to the organelle genome [74]. We used REDITools software to detect potential RNA editing sites in PCG with parameter settings of coverage ≥5, frequency ≥0.1, and p-value ≤0.5 [75]. Tablet v1.17.08.17 software was used to analyze the BAM files and manually identify and remove false-positive RNA editing events [76].

Identification of plastid transfer sequence

Online BLAST software was used to perform homology comparisons between the cpDNA and mtDNA of *C. stoloniferus* with parameter settings of word size 7 and E value=$1e^{-5}$. We analyzed homologous sequence regions and identified the sequence length, quantity, and gene types of MTPT while focusing only on sequences exceeding 50 bp and containing gene transfer sequences. Advanced Circos in the TBtools software was used to draw chloroplast and mitochondrial DNA sequence transfer maps [77, 78].

Construction of phylogenetic tree

The mtDNA and cpDNA sequences of closely related species were downloaded from

510 the NCBI website (https://www.ncbi.nlm.nih.gov), and 27 and 68 PCGs shared by the
511 mtDNA and cpDNA of 11 species, respectively, were identified (Tables S19 and S20).
512 Based on the amino acid sequences of the shared genes, the ML method of the MEGA11
513 software [79] was used to construct phylogenetic trees with a bootstrap value of 1,000
514 and an evolutionary model of GTR+I+G.

515 **Comparative analysis of organelle genomes in closely related species**

516 Using BLAST software, the mtDNA and cpDNA of the four sedge plants were
517 compared pairwise with the parameter E value=$1e^{-10}$. Homologous sequence lengths of
518 greater than 40 bp were used as conserved regions for the organelle genome collinearity
519 analysis. Using the KaKs Calculator v2.0 software [32], we calculated the Ka/Ks values
520 of the PCG and rRNA genes in the organelle genomes of nine closely related species
521 through pairwise comparison. When the Ka or Ks values were zero, they were not
522 included in the statistics. Using Mafft software for gene nucleotide sequence multiple
523 alignment, DnaSP v5.10 software [80] was used to calculate the Pi value of the gene
524 and visualize the calculation results as a box plot using Origin2019.

525 **Abbreviations**

526 cpDNA Chloroplast genome

527 mtDNA Mitochondrial genome

528 MTPT Mitochondrial plastid sequence

529 PCG Protein coding gene

530 RSCU Relative synonymous codon usage

531 SSR Simple sequence repeat

Supplementary Information

The online version contains supplementary material available at…

Acknowledgements

We greatly appreciate Shenzhen Huitong Biotechnology Co., Ltd., China, for genome sequencing and data analysis services and Editage for English language editing.

Authors' contributions

A.W. and J.N. conceived and designed the experiments. X.M. conducted the experiments and wrote the manuscript. D.L. and J.L. collected genomic data and created charts. W.Y. verified the genome splicing. X.D. and L.H. reviewed and revised the manuscript. All authors have read and agreed to the final version of this manuscript.

Funding

This work was supported by grants from the Natural Science Foundation of Guangxi (2021GXNSFAA196061), the Natural Science Foundation of China (32360542, 32260680), the Nanning Enterprise Horizontal Project (BB33100281), the National Key Research and Guangxi Zhuang Autonomous Region Development Plan Project (AB22080090), the Provincial Undergraduate Training Program for Innovation and Entrepreneurship (202310606042), the China Agricultural Research System (CARS-21) of the Ministry of Finance and the National Agricultural Research Center.

Availability of data and materials

The raw sequencing data and assembly sequences of *C. stoloniferus* have been deposited in NCBI with accession numbers PRJNA759403, SRR15684162, SRR15684161, MZ930067, MZ930068 and MZ895087, respectively. The BioSample

numbers related to the raw transcriptome data of *C. stoloniferus* leaves were SAMN39414344, SAMN39414345, and SAMN3941346.

Declarations

Ethics approval and consent to participate

The collection of plant materials complied with all relevant institutional, national, and international guidelines. As *C. stoloniferus* is not an endangered wild plant, plant collection does not require specific permits.

Consent for publication

Not applicable.

Competing interests

The authors declare have no competing interests.

References

1. Hayasaka D, Fujiwara K, Box EO. Recovery of sandy beach and maritime forest vegetation on Phuket Island (Thailand) after the major Indian Ocean tsunami of 2004. Appl. Veg. Sci. 2009;12(2):211–224. https://doi.org/10.1111/j.1654-109X.2009.01017.x.
2. Dávid CZ, Hohmann J, Vasas A. Chemistry and pharmacology of Cyperaceae stilbenoids: a review. Molecules. 2021;26(9):2794. https://doi.org/10.3390/molecules26092794.
3. Chau NM, Hong Hanh TT, Luyen NT, et al. Flavanones and stilbenes from *Cyperus stoloniferus* Retz. Biochem. Syst. Ecol. 2013;50:220–222. https://doi.org/10.1016/j.bse.2013.04.004.
4. Kumar, B. *Cyperus Stoloniferus*: The IUCN Red List of Threatened Species 2013: E.T177286A7406040, 2010; https://doi.org/10.2305/IUCN.UK.2011-1.RLTS.T177286A7406040.en.
5. Muasya AM, Reynders M, Goetghebeur P, et al. *Dracoscirpoides* (Cyperaceae) — a new genus from Southern Africa, its taxonomy and floral ontogeny. South Afr. J. Bot. 2012;78:104–115. https://doi.org/10.1016/j.sajb.2011.05.011.
6. Semmouri I, Bauters K, Léveillé-Bourret É, et al. Phylogeny and systematics of Cyperaceae, the evolution and importance of embryo morphology. Bot. Rev. 2019;85(1):1–39. https://doi.org/10.1007/s12229-018-9202-0.
7. Alves L, Prata A, Edson B, et al. Ligule and contraligule in Cyperaceae: A systematic review. South Afr. J. Bot. 2023;157:372–379. https://doi.org/10.1016/j.sajb.2023.04.011.
8. Larridon I, Zuntini AR, Léveillé É, et al. A new classification of Cyperaceae (Poales) supported by phylogenomic data. J. Syst. Evol. 2021;59(4):852–895. https://doi.org/10.1111/jse.12757.
9. Larridon I, Bauters K, Reynders M, et al. Towards a new classification of the

giant paraphyletic genus *Cyperus* (Cyperaceae): phylogenetic relationships and generic delimitation in C $_4$ *Cyperus*: C $_4$ *Cyperus* Phylogeny (Cyperaceae). Bot. J. Linn. Soc. 2013;172(1):106–126. https://doi.org/10.1111/boj.12020.

10. Villaverde T, Jiménez P, Luceño M, et al. A new classification of *Carex* (Cyperaceae) subgenera supported by a HybSeq backbone phylogenetic tree. Bot. J. Linn. Soc. 2020;194(2):141–163. https://doi.org/10.1093/botlinnean/boaa042.
11. Starr JR, Jiménez P, Zuntini AR, et al. Targeted sequencing supports morphology and embryo features in resolving the classification of Cyperaceae tribe Fuireneae s.l. J. Syst. Evol. 2021;59(4):809–832. https://doi.org/10.1111/jse.12721.
12. Hipp AL. Nonuniform processes of chromosome evolution in sedges (carex: cyperaceae). Evolution. 2007;61(9):2175–2194. https://doi.org/10.1111/j.1558-5646.2007.00183.x.
13. Márquez JI, Martín S, Jiménez P, et al. Macroevolutionary insights into sedges (*Carex*: Cyperaceae): the effects of rapid chromosome number evolution on lineage diversification. J. Syst. Evol. 2021;59(4):776–790. https://doi.org/10.1111/jse.12730.
14. Niu L, Zhang Y, Yang C, et al. Complete mitochondrial genome sequence and comparative analysis of the cultivated yellow nutsedge. Plant Genome. 2022;15(3):e20239. https://doi.org/10.1002/tpg2.20239.
15. Xu S, Teng K, Zhang H, et al. The first complete mitochondrial genome of *Carex* (*C. breviculmis*): a significantly expanded genome with highly structural variations. Planta. 2023;258(2):43. https://doi.org/10.1007/s00425-023-04169-1.
16. Huang X, Coulibaly D, Tan W, et al. The analysis of genetic structure and characteristics of the chloroplast genome in different Japanese apricot germplasm populations. BMC Plant Biol. 2022;22(1):354. https://doi.org/10.1186/s12870-022-03731-5.
17. Dong S, Ying Z, Yu S, et al. Complete chloroplast genome of *Stephania tetrandra*

(Menispermaceae) from Zhejiang Province: insights into molecular structures, comparative genome analysis, mutational hotspots and phylogenetic relationships. BMC Genomics. 2021;22(1):880. https://doi.org/10.1186/s12864-021-08193-x.

18. Li YX, Li ZH, Schuiteman A, et al. Phylogenomics of Orchidaceae based on plastid and mitochondrial genomes. Mol. Phylogenet. Evol. 2019;139:106540. https://doi.org/10.1016/j.ympev.2019.106540.

19. Wick RR, Schultz MB, Zobel J, et al. Bandage: interactive visualization of *de novo* genome assemblies. Bioinformatics. 2015;31(20):3350–3352. https://doi.org/10.1093/bioinformatics/btv383.

20. He ZS, Zhu A, Yang JB, et al. Organelle genomes and transcriptomes of nymphaea reveal the interplay between Intron splicing and RNA Editing. Int. J. Mol. Sci. 2021;22(18):9842. https://doi.org/10.3390/ijms22189842.

21. Liao X, Zhu W, Zhou J, et al. Repetitive DNA sequence detection and its role in the human genome. Commun. Biol. 2023;6(1):954. https://doi.org/10.1038/s42003-023-05322-y.

22. Shapiro JA, Von Sternberg R. Why repetitive DNA is essential to genome function. Biol. Rev. 2005;80(2):227–250. https://doi.org/10.1017/S1464793104006657.

23. De Bustos A, Cuadrado A, Jouve N. Sequencing of long stretches of repetitive DNA. Sci. Rep. 2016;6(1):36665. https://doi.org/10.1038/srep36665.

24. Athey J, Alexaki A, Osipova E, et al. A new and updated resource for codon usage tables. BMC Bioinformatics. 2017;18(1):391. https://doi.org/10.1186/s12859-017-1793-7.

25. Zhou P, Zhang Q, Li F, et al. Assembly and comparative analysis of the complete mitochondrial genome of *Ilex metabaptista* (Aquifoliaceae), a Chinese endemic species with a narrow distribution. BMC Plant Biol. 2023;23(1):393. https://doi.org/10.1186/s12870-023-04377-7.

26. Li Y, Gu M, Liu X, et al. Sequencing and analysis of the complete mitochondrial

646 genomes of *Toona sinensis* and *Toona ciliata* reveal evolutionary features of Toona.
647 BMC Genomics. 2023;24(1):58. https://doi.org/10.1186/s12864-023-09150-6.
648 27. Castandet B, Araya A. RNA editing in plant organelles. Why make it easy?
649 Biochem. Mosc. 2011;76(8):924–931.
650 https://doi.org/10.1134/S0006297911080086.
651 28. Wang D, Wu YW, Shih AC, et al. Transfer of chloroplast genomic DNA to
652 mitochondrial genome occurred at least 300 MYA. Mol. Biol. Evol.
653 2007;24(9):2040–2048. https://doi.org/10.1093/molbev/msm133.
654 29. Alverson AJ, Wei X, Rice DW, et al. Insights into the evolution of mitochondrial
655 genome size from complete sequences of *Citrullus lanatus* and *Cucurbita pepo*
656 (Cucurbitaceae). Mol. Biol. Evol. 2010;27(6):1436–1448.
657 https://doi.org/10.1093/molbev/msq029.
658 30. Wicke S, Schneeweiss GM, dePamphilis CW, et al. The evolution of the plastid
659 chromosome in land plants: gene content, gene order, gene function. Plant Mol.
660 Biol. 2011;76(3–5):273–297. https://doi.org/10.1007/s11103-011-9762-4.
661 31. Bi Y, Zhang M, Xue J, et al. Chloroplast genomic resources for phylogeny and
662 DNA barcoding: a case study on Fritillaria. Sci. Rep. 2018;8(1):1184.
663 https://doi.org/10.1038/s41598-018-19591-9.
664 32. Wang D, Zhang Y, Zhang Z, et al. KaKs_Calculator 2.0: a toolkit incorporating
665 gamma-series methods and sliding window strategies. Genomics Proteomics
666 Bioinformatics. 2010;8(1):77–80. https://doi.org/10.1016/S1672-0229(10)60008-3.
667 33. Plancarte DC, Solórzano S. Structural and gene composition variation of the
668 complete mitochondrial genome of *Mammillaria huitzilopochtli* (Cactaceae,
669 Caryophyllales), revealed by de novo assembly. BMC Genomics. 2023;24(1):509.
670 https://doi.org/10.1186/s12864-023-09607-8.
671 34. Ni Y, Li J, Chen H, et al. Comparative analysis of the chloroplast and
672 mitochondrial genomes of *Saposhnikovia divaricata* revealed the possible transfer

673 of plastome repeat regions into the mitogenome. BMC Genomics. 2022;23(1):570.
674 https://doi.org/10.1186/s12864-022-08821-0.
675 35. Daniell H, Lin CS, Yu M, et al. Chloroplast genomes: diversity, evolution, and
676 applications in genetic engineering. Genome Biol. 2016;17(1):134.
677 https://doi.org/10.1186/s13059-016-1004-2.
678 36. Wu R, Yu C, Wu Y. Characterization of the complete plastome of *Cyperus*
679 *rotundus* L. (Cyperaceae). Mitochondrial DNA Part B. 2021;6(1):58–59.
680 https://doi.org/10.1080/23802359.2020.1845999.
681 37. Ren W, Guo D, Xing G, et al. Complete chloroplast genome sequence and
682 comparative and phylogenetic analyses of the cultivated *Cyperus esculentus*.
683 Diversity. 2021;13(9):405. https://doi.org/10.3390/d13090405.
684 38. Feng L, Wang Z, Wang C, et al. Multichromosomal mitochondrial genome of
685 *Punica granatum*: comparative evolutionary analysis and gene transformation from
686 chloroplast genomes. BMC Plant Biol. 2023;23(1):512.
687 https://doi.org/10.1186/s12870-023-04538-8.
688 39. Kozik A, Rowan BA, Lavelle D, et al. The alternative reality of plant mitochondrial
689 DNA: one ring does not rule them all. PLOS Genet. 2019;15(8):e1008373.
690 https://doi.org/10.1371/journal.pgen.1008373.
691 40. Jackman SD, Coombe L, Warren RL, et al. Complete mitochondrial genome of
692 a gymnosperm, Sitka Spruce (*Picea sitchensis*), indicates a complex physical
693 structure. Genome Biol. Evol. 2020;12(7):1174–1179.
694 https://doi.org/10.1093/gbe/evaa108.
695 41. Xia C, Li J, Zuo Y, et al. Complete mitochondrial genome of *Thuja sutchuenensis*
696 and its implications on evolutionary analysis of complex mitogenome architecture
697 in Cupressaceae. BMC Plant Biol. 2023;23(1):84. https://doi.org/10.1186/s12870-
698 023-04054-9.
699 42. Zhang F, Li W, Gao C, et al. Deciphering tea tree chloroplast and mitochondrial

genomes of *Camellia sinensis* var. *assamica*. Sci. Data. 2019;6(1):209. https://doi.org/10.1038/s41597-019-0201-8.

43. Zhong F, Ke W, Li Y, et al. Comprehensive analysis of the complete mitochondrial genomes of three *Coptis* species (*C. chinensis*, *C. deltoidea* and *C. omeiensis*): the important medicinal plants in China. Front. Plant Sci. 2023;14:1166420. https://doi.org/10.3389/fpls.2023.1166420.

44. Kim CK, Kim YK. The multipartite mitochondrial genome of *Fallopia multiflora* (Caryophyllales: Polygonaceae). Mitochondrial DNA Part B. 2018;3(1):155–156. https://doi.org/10.1080/23802359.2018.1437796.

45. Sun Z, Wu Y, Fan P, et al. Assembly and analysis of the mitochondrial genome of *Prunella vulgaris*. Front. Plant Sci. 2023;14:1237822. https://doi.org/10.3389/fpls.2023.1237822.

46. Logacheva MD, Schelkunov MI, Fesenko AN, et al. Mitochondrial genome of *Fagopyrum esculentum* and the genetic diversity of extranuclear genomes in buckwheat. Plants. 2020;9(5):618. https://doi.org/10.3390/plants9050618.

47. Shan Y, Li J, Zhang X, et al. The complete mitochondrial genome of *Amorphophallus albus* and development of molecular markers for five Amorphophallus species based on mitochondrial DNA. Front. Plant Sci. 2023;14:1180417. https://doi.org/10.3389/fpls.2023.1180417.

48. Han H, Qiu R, Liu Y, et al. Analysis of chloroplast genomes provides insights into the evolution of *Agropyron*. Front. Genet. 2022;13:832809. https://doi.org/10.3389/fgene.2022.832809.

49. Janouškovec J, Liu S-L, Martone PT, et al. Evolution of red algal plastid genomes: ancient architectures, introns, horizontal gene transfer, and taxonomic utility of plastid markers. PLoS ONE. 2013;8(3):e59001. https://doi.org/10.1371/journal.pone.0059001.

50. Kan SL, Shen TT, Ran JH, et al. Both Conifer II and Gnetales are characterized

727 by a high frequency of ancient mitochondrial gene transfer to the nuclear genome.
728 BMC Biol. 2021;19(1):146. https://doi.org/10.1186/s12915-021-01096-z.
729 51. Brožová V，Proćków J，Záveská DL. Toward finally unraveling the phylogenetic
730 relationships of Juncaceae with respect to another cyperid family, Cyperaceae. Mol.
731 Phylogenet. Evol. 2022;177:107588. https://doi.org/10.1016/j.ympev.2022.107588.
732 52. Elliott TL，Spalink D，Larridon I，et al. Global analysis of Poales diversification
733 – parallel evolution in space and time into open and closed habitats. New Phytol.
734 2023;nph.19421. https://doi.org/10.1111/nph.19421.
735 53. Niemeyer PW，Irisarri I，Scholz P，et al. A seed-like proteome in oil-rich tubers.
736 Plant J. 2022;112(2):518–534. https://doi.org/10.1111/tpj.15964.
737 54. Yuan J，Zhang X，Wang M，et al. Simple sequence repeats drive genome plasticity
738 and promote adaptive evolution in penaeid shrimp. Commun. Biol. 2021;4(1):186.
739 https://doi.org/10.1038/s42003-021-01716-y.
740 55. Yang Y，Jia Y，Zhao Y，et al. Comparative chloroplast genomics provides insights
741 into the genealogical relationships of endangered *Tetraena mongolica* and the
742 chloroplast genome evolution of related *Zygophyllaceae* species. Front. Genet.
743 2022;13:1026919. https://doi.org/10.3389/fgene.2022.1026919.
744 56. Wang YJ，Liu JQ，Miehe G. Phylogenetic origins of the Himalayan endemic
745 *Dolomiaea*, *Diplazoptilon* and *Xanthopappus* (Asteraceae: Cardueae) based on
746 three DNA regions. Ann. Bot. 2007;99(2):311–322.
747 https://doi.org/10.1093/aob/mcl259.
748 57. Choi KS，Park S. Complete plastid and mitochondrial genomes of *Aeginetia indica*
749 reveal intracellular gene transfer (IGT), horizontal gene transfer (HGT), and
750 cytoplasmic male sterility (CMS). Int. J. Mol. Sci. 2021;22(11):6143.
751 https://doi.org/10.3390/ijms22116143.
752 58. Timmis JN，Ayliffe MA，Huang CY，et al. Endosymbiotic gene transfer: organelle
753 genomes forge eukaryotic chromosomes. Nat. Rev. Genet. 2004;5(2):123–135.

https://doi.org/10.1038/nrg1271.

59. Bergthorsson U，Adams KL，Thomason B，et al. Widespread horizontal transfer of mitochondrial genes in flowering plants. Nature. 2003;424(6945):197–201. https://doi.org/10.1038/nature01743.

60. Hao W，Liu G，Wang W，et al. RNA editing and its roles in plant organelles. Front. Genet. 2021;12:757109. https://doi.org/10.3389/fgene.2021.757109.

61. Ichinose M，Sugita M. RNA Editing and its molecular mechanism in plant Organelles. Genes. 2016;8(1):5. https://doi.org/10.3390/genes8010005.

62. Small ID，Schallenberg M，Takenaka M，et al. Plant organellar RNA editing: what 30 years of research has revealed. Plant J. 2020;101(5):1040–1056. https://doi.org/10.1111/tpj.14578.

63. Zhang A，Fang J，Zhang X. Diversity of RNA editing in chloroplast transcripts across three main plant clades. Plant Syst. Evol. 2023;309(2):12. https://doi.org/10.1007/s00606-023-01849-z.

64. Fan W，Guo W，Funk L，et al. Complete loss of RNA editing from the plastid genome and most highly expressed mitochondrial genes of *Welwitschia mirabilis*. Sci. China Life Sci. 2019;62(4):498–506. https://doi.org/10.1007/s11427-018-9450-1.

65. Cheng Y，He X，Priyadarshani SVGN，et al. Assembly and comparative analysis of the complete mitochondrial genome of *Suaeda glauca*. BMC Genomics. 2021;22(1):167. https://doi.org/10.1186/s12864-021-07490-9.

66. Kabala AM，Binko K，Godard F，et al. Assembly-dependent translation of subunits *6* (*Atp6*) and *9* (*Atp9*) of ATP synthase in yeast mitochondria. Genetics. 2022;220(3):iyac007. https://doi.org/10.1093/genetics/iyac007.

67. Bietenhader M，Martos A，Tetaud E，et al. Experimental relocation of the mitochondrial *ATP9* gene to the nucleus reveals forces underlying mitochondrial genome evolution. PLoS Genet. 2012;8(8):e1002876.

781 https://doi.org/10.1371/journal.pgen.1002876.
782 68. Han K, Shi C, Li L, et al. Lineage-specific evolution of mangrove plastid genomes.
783 Plant Genome. 2020;13(2):e20019. https://doi.org/10.1002/tpg2.20019.
784 69. Abdel-Latif A, Osman G. Comparison of three genomic DNA extraction methods
785 to obtain high DNA quality from maize. Plant Methods. 2017;13(1):1.
786 https://doi.org/10.1186/s13007-016-0152-4.
787 70. Patel RK, Jain M. NGS QC toolkit: a toolkit for quality control of next generation
788 sequencing data. PLoS ONE. 2012;7(2):e30619.
789 https://doi.org/10.1371/journal.pone.0030619.
790 71. Ruby JG, Bellare P, DeRisi JL. PRICE: software for the targeted assembly of
791 components of (Meta) genomic sequence data. G3 GenesGenomesGenetics.
792 2013;3(5):865–880. https://doi.org/10.1534/g3.113.005967.
793 72. Bankevich A, Nurk S, Antipov D, et al. SPAdes: a new genome assembly
794 algorithm and its applications to single-cell sequencing. J. Comput. Biol.
795 2012;19(5):455–477. https://doi.org/10.1089/cmb.2012.0021.
796 73. Benson G. Tandem repeats finder: a program to analyze DNA sequences. Nucleic
797 Acids Res. 1999;27(2):573–580. https://doi.org/10.1093/nar/27.2.573.
798 74. Kim D, Pertea G, Trapnell C, et al. TopHat2: accurate alignment of transcriptomes
799 in the presence of insertions, deletions and gene fusions. Genome Biol.
800 2013;14(4):R36. https://doi.org/10.1186/gb-2013-14-4-r36.
801 75. Picardi E, Pesole G. REDItools: high-throughput RNA editing detection made easy.
802 Bioinformatics. 2013;29(14):1813–1814.
803 https://doi.org/10.1093/bioinformatics/btt287.
804 76. Milne I, Stephen G, Bayer M, et al. Using ablet for visual exploration of second-
805 generation sequencing data. Brief. Bioinform. 2013;14(2):193–202.
806 https://doi.org/10.1093/bib/bbs012.
807 77. Zhang H, Meltzer P, Davis S. RCircos: an R package for circos 2D track plots.

808 BMC Bioinformatics. 2013;14(1):244. https://doi.org/10.1186/1471-2105-14-244.
809 78. Chen C，Chen H，Zhang Y，et al. TBtools: an integrative toolkit developed for
810 interactive analyses of big biological data. Mol. Plant. 2020;13(8):1194–1202.
811 https://doi.org/10.1016/j.molp.2020.06.009.
812 79. Tamura K，Stecher G，Kumar S. MEGA11: Molecular evolutionary genetics
813 analysis version 11. Mol. Biol. Evol. 2021;38(7):3022–3027.
814 https://doi.org/10.1093/molbev/msab120.
815 80. Librado P，Rozas J. DnaSP v5: a software for comprehensive analysis of DNA
816 polymorphism data. Bioinformatics. 2009;25(11):1451–1452.
817 https://doi.org/10.1093/bioinformatics/btp187.

Fig. 1 Contig splicing and PCR amplification detection of *C. stoloniferus* mtDNA. (A) The mtDNA consists of two independent circular DNA, including mt1 and mt2. (B) mt2 consists of four contig overlapping groups, among which contig2 is a 15,034bp reverse repeating direction. The counterclockwise arrow indicates a forward repeating sequence, while the clockwise arrow indicates a reverse repeating sequence. (C) Agarose gel electrophoresis of PCR amplification products of four overlapping regions (P1, P2, P3 and P4). (D) Four hypothetical types of contig splicing combinations that do not exist in mt2.

Fig. 2 Circular DNA map of the organelle genome in *C. stoloniferus*. Different functional groups of genes are represented by different colors

Fig. 3 The repetitive sequence of the organelle genome in *C. stoloniferus*. (A) The short lines in the outer, middle, and inner circles represent the positions of SSRs, tandem repeats, and dispersed repeats in the organelle genome, respectively. (B) The types and quantities of SSRs. (C) The types and quantities of tandem repeats and dispersed repeats

Fig. 4 Relative synonymous codon usage (RSCU) of the organelle genome in *C. stoloniferus*. (A) RSCU analysis of cpDNA. (B) RSCU analysis of mtDNA

Fig. 5 Distribution of RNA editing sites in the organelle genome PCGs of *C. stoloniferus*

Fig. 7 The phylogenetic relationship between *C. stoloniferus* and 10 other species. (A) and (B) are phylogenetic trees constructed based on genes shared by 27 mitochondria (Table S19) and 68 chloroplasts (Table S20), respectively. Color represents plants of the same family

Fig. 8 The collinear blocks between the organelle genomes of four species in Cyperaceae. (A) and (B) are collinear blocks of mtDNA and cpDNA, respectively. The bar chart represents the organelle genome, and the arc represents the homologous sequence of adjacent species. The red highlighted area represents homologous segments with a length greater than 500 bp and an E value of 0, while the gray area represents regions with good homology

Fig. 9 Nucleotide diversity of genes in organelle genomes of 9 closely related species. (A) The Pi value of mitochondrial genes. (B) and (C) indicate the Pi values of chloroplast genes

Fig. 10 Ka/Ks analysis of PCGs in the organelle genomes of 9 closely related species. (A) The Ka/Ks of mitochondrial PCGs. (B) and (C) indicate the Ka/Ks of chloroplast PCGs

Table 1 The size, base content, and gene composition of organelle genomes in *C. stoloniferus*

Table 2 Gene composition of mtDNA in *C. stoloniferus.* The superscript numbers in parentheses represent gene copy numbers, and * indicates that the gene contains intron

856

Fig. 1 Contig splicing and PCR amplification detection of *C. stoloniferus* mtDNA. (A) The mtDNA consists of two independent circular DNA, including mt1 and mt2. (B) mt2 consists of four contig overlapping groups, among which contig2 is a 15,034bp reverse repeating direction. The counterclockwise arrow indicates a forward repeating sequence, while the clockwise arrow indicates a reverse repeating sequence. (C) Agarose gel electrophoresis of PCR amplification products of four overlapping regions (P1, P2, P3 and P4). (D) Four hypothetical types of contig splicing combinations that do not exist in mt2

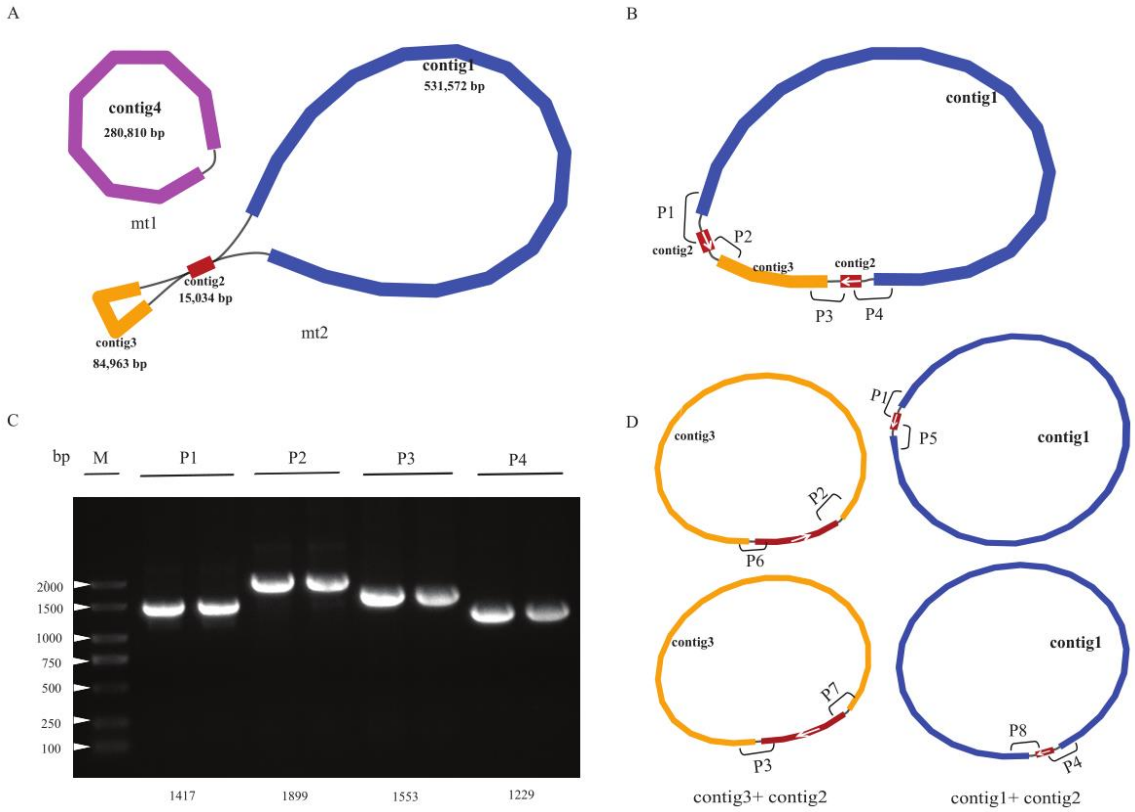

Fig. 2 Circular DNA map of the organelle genome in *C.stoloniferus*. Different functional groups of genes are represented by different colors

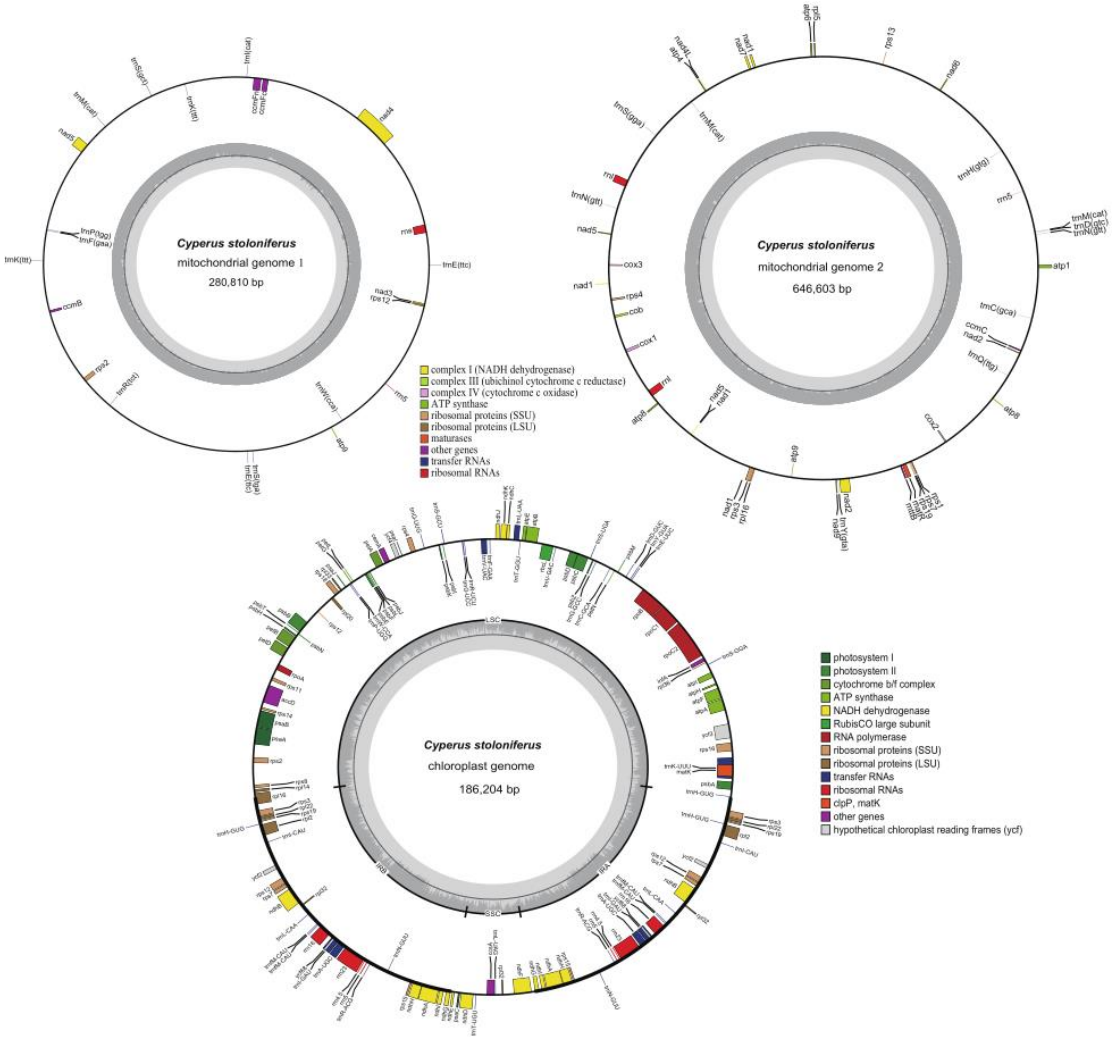

Fig. 3 The repetitive sequence of the organelle genome in *C.stoloniferus*. (A) The short lines in the outer, middle, and inner circles represent the positions of SSRs, tandem repeats, and dispersed repeats in the organelle genome, respectively. (B) The types and quantities of SSRs. (C) The types and quantities of tandem repeats and dispersed repeats

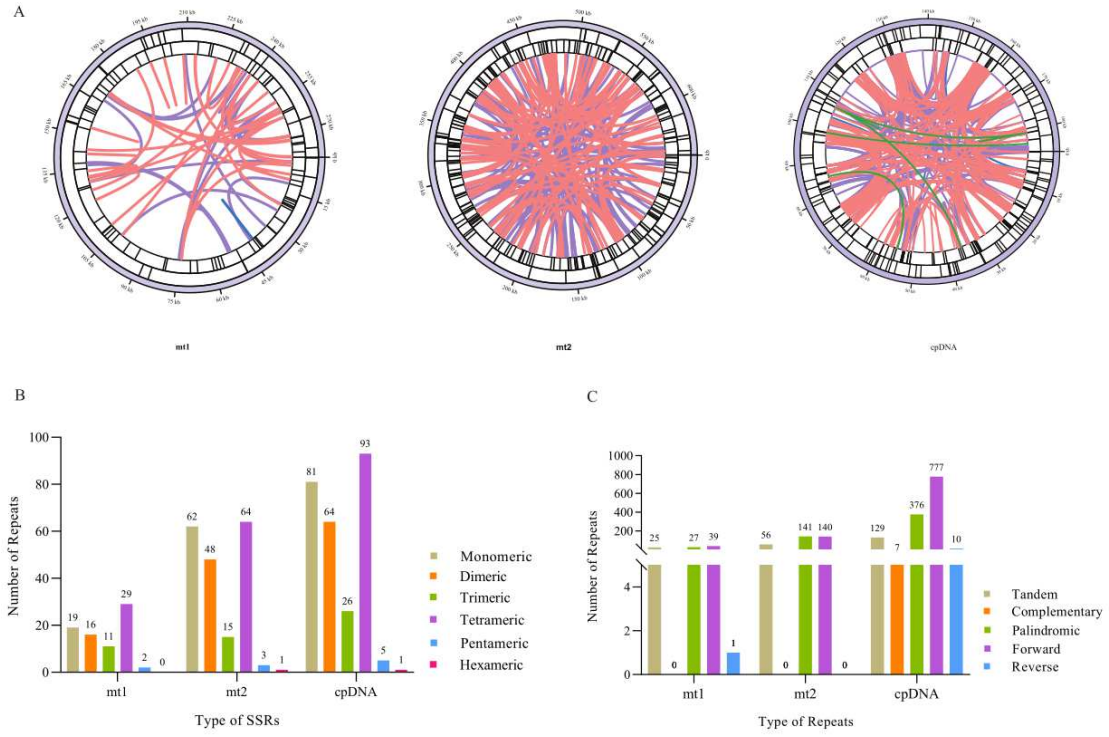

Fig. 4 Relative synonymous codon usage (RSCU) of the organelle genome in *C. stoloniferus*. (A) RSCU analysis of cpDNA. (B) RSCU analysis of mtDNA

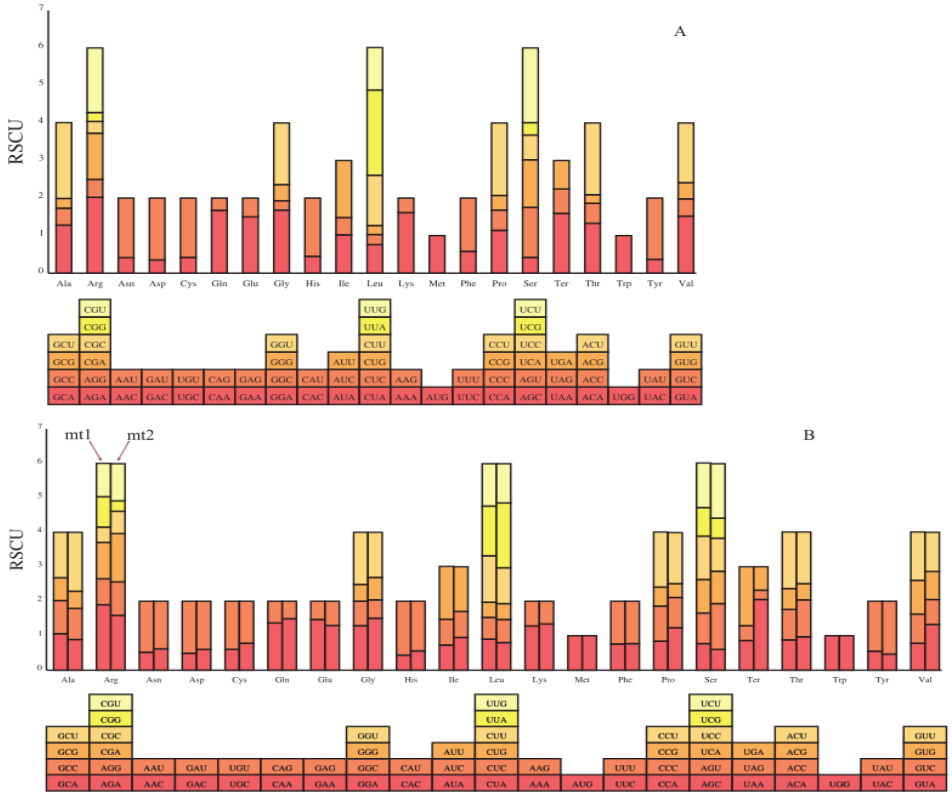

Fig. 5 Distribution of RNA editing sites in the organelle genome PCGs of *C. stoloniferus*

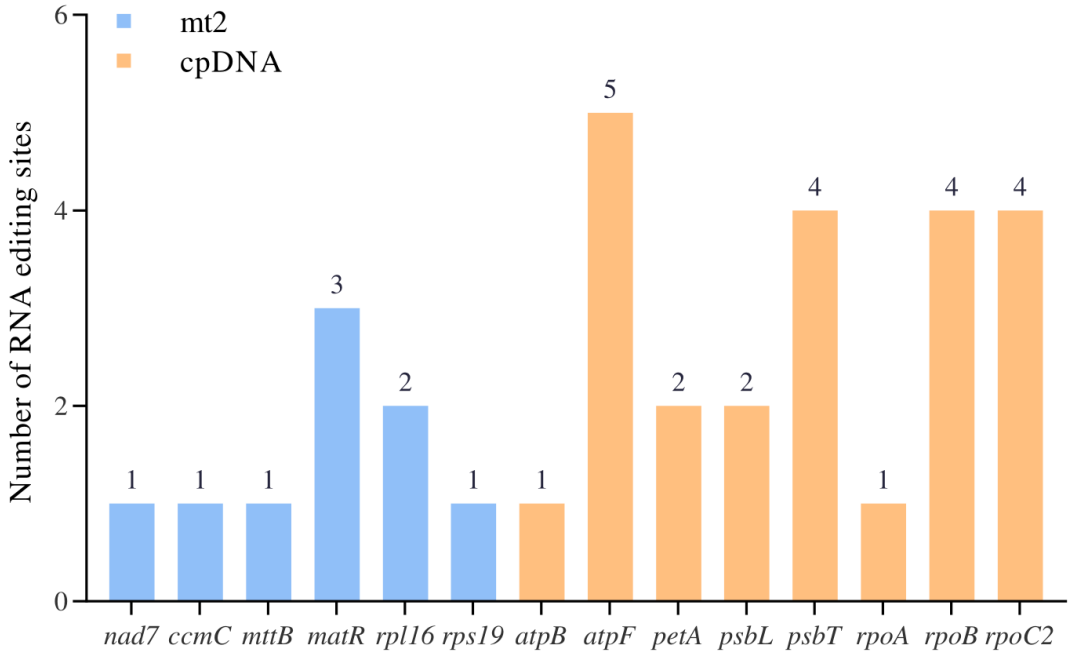

Fig. 6 Transfer events of plastid DNA to the mitochondrial genome in *C. stoloniferus*. The outer arc represents mt1, mt2, and cpDNA, while the inner arc represents the

corresponding transfer MTPTs

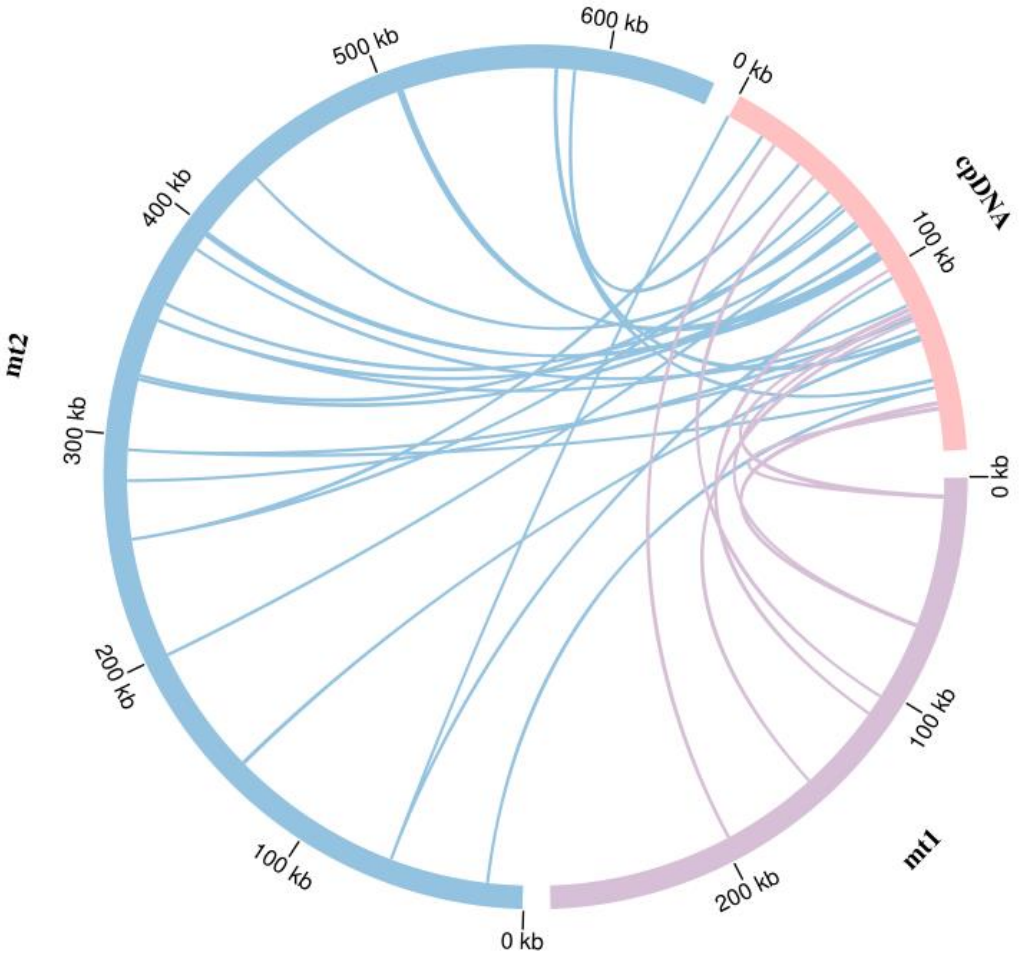

Fig. 7 The phylogenetic relationship between *C. stoloniferus* and 10 other species. (A) and (B) are phylogenetic trees constructed based on genes shared by 27 mitochondria

(Table S19) and 68 chloroplasts (Table S20), respectively. Color represents plants of the same family

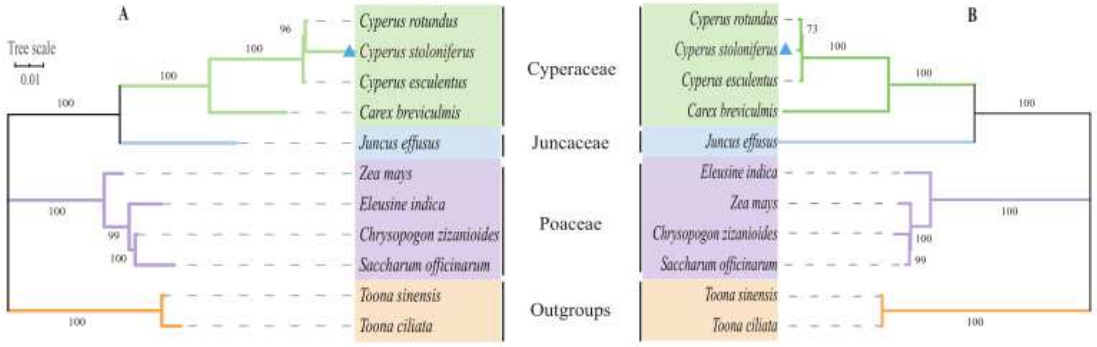

Fig. 8 The collinear blocks between the organelle genomes of four species in Cyperaceae. (A) and (B) are collinear blocks of mtDNA and cpDNA, respectively. The

bar chart represents the organelle genome, and the arc represents the homologous sequence of adjacent species. The red highlighted area represents homologous segments with a length greater than 500 bp and an E value of 0, while the gray area represents regions with good homology

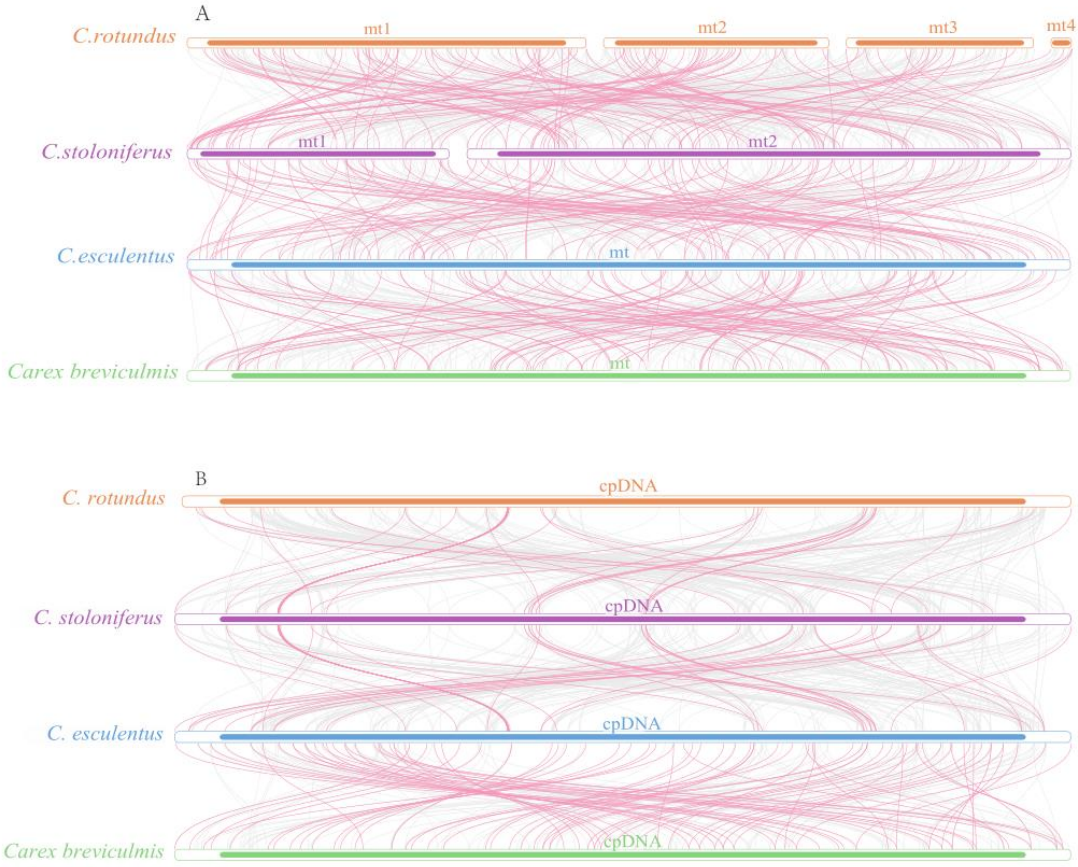

Fig. 9 Nucleotide diversity of genes in organelle genomes of 9 closely related species. (A) The Pi value of mitochondrial genes. (B) and (C) indicate the Pi values of

chloroplast genes

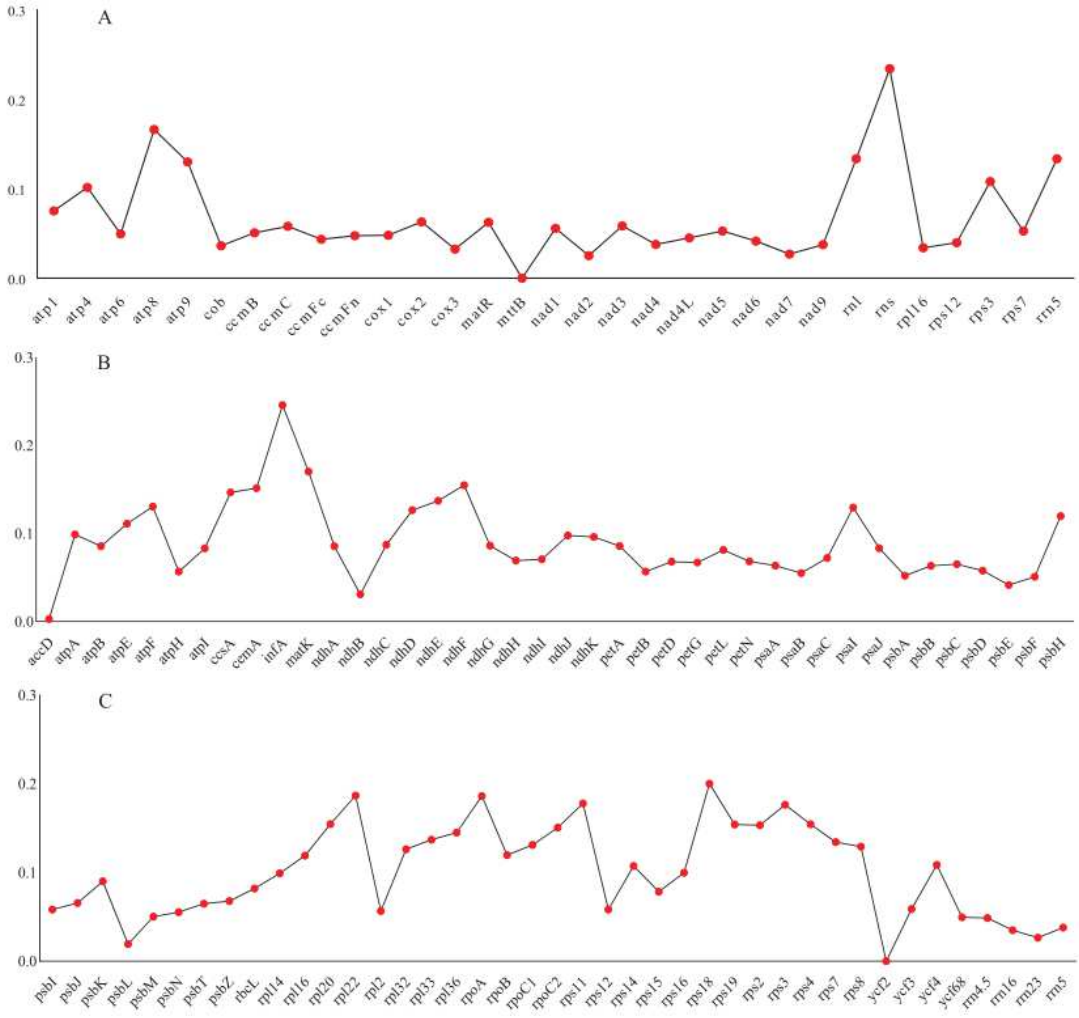

Fig. 10 Ka/Ks analysis of PCGs in the organelle genomes of 9 closely related species. (A) The Ka/Ks of mitochondrial PCGs. (B) and (C) indicate the Ka/Ks of chloroplast

PCGs

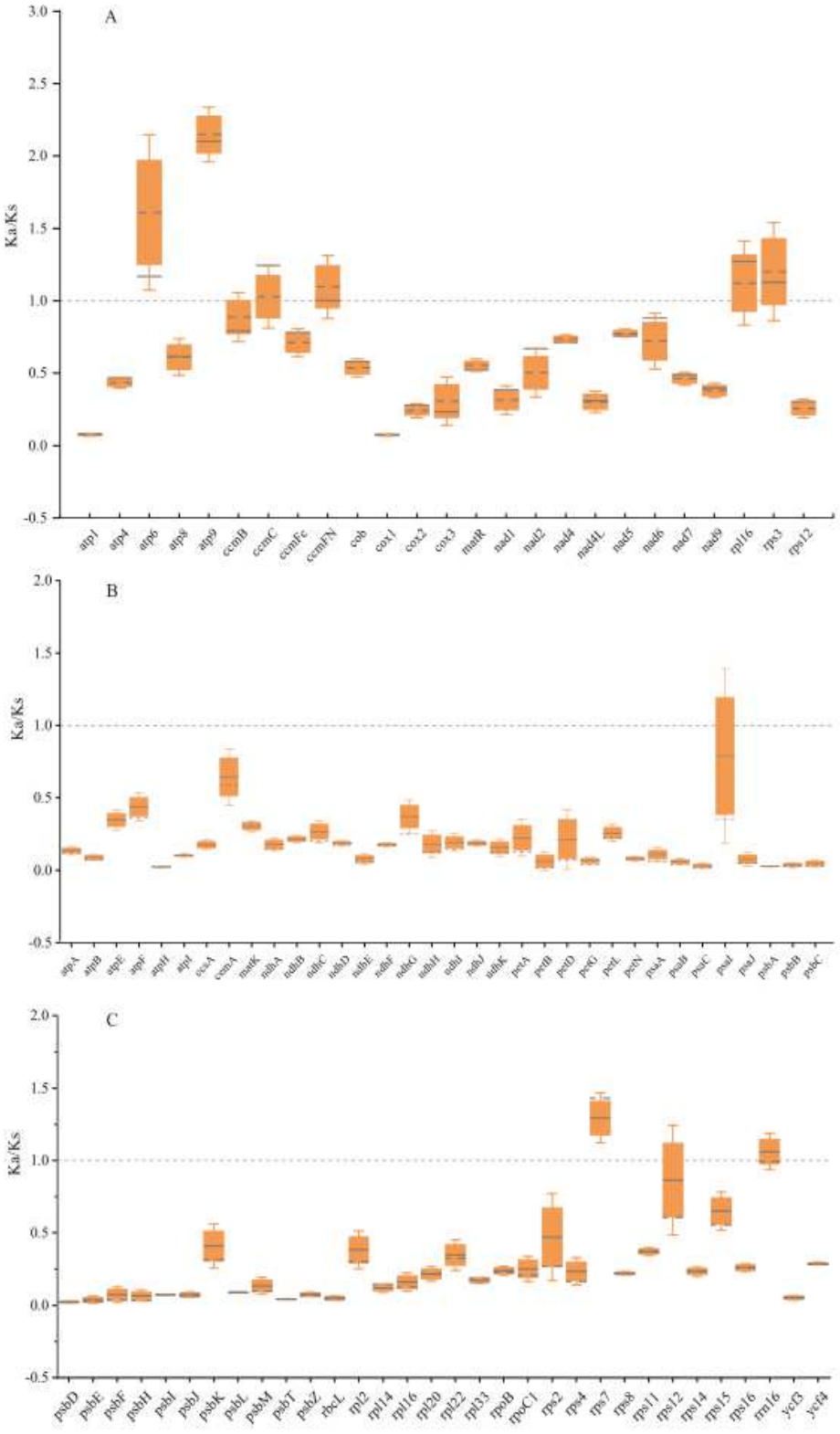

Table 1 The size, base content, and gene composition of organelle genomes in *C. stoloniferus*

Genome	Size (bp)	A%	T%	G%	C%	PCG	rRNA	tRNA	Accession number
mt1	280,810	29.61	29.80	20.41	20.19	9	2	12	MZ930067
mt2	646,603	29.89	29.54	20.45	20.14	28	3	10	MZ930068
cpDNA	186,204	33.20	33.61	16.23	16.96	93	8	40	MZ895087

Table 2 Gene composition of mtDNA in *C. stoloniferus*

Group of genes	mt1	mt2

Complex I	*nad3*, *nad4**, *nad5**	*nad1**, *nad2**, *nad4L*, *nad6*, *nad5**, *nad7*, *nad9*
Complex III		*cob*
Complex IV		*cox1*, *cox2*, *cox3*
ATP synthase	*atp9*	*atp1*, *atp4*, *atp6*, *atp8*(2), *atp9*
Ribusomal protein large subunit (LSU)		*rpl5*, *rpl16*, *rps19*, *rps7*
Ribosomal protein small subunit (SSU)	*rps2*, *rps12*	*rps1*, *rps3**, *rps4*, *rps13*
Maturases		*matR*
Other genes	*ccmB*, *ccmFc*, *ccmFN*	*ccmC*, *mttB*
Ribosomal RNA (rRNA)	*rns*, *rrn5*	*rnl*(2), *rrn5*
Transfer RNA (tRNA)	*trnE-TTC*(2), *trnF-GAA*, *trnI-CAT*, *trnK-TTT*(2), *trnM-CAT*, *trnP-TGG*, *trnR-TCT*, *trnS-GCT*, *trnS-TGA*, *trnW-CCA*	*trnC-GCA*, *trnD-GTC*, *trnH-GTG*, *trnM-CAT*(2), *trnN-GTT*, *trnN-GTT*, *trnQ-TTG*, *trnS-GGA*, *trnY-GTA*

Note: The numbers in parentheses indicate the number of the gene, and * indicates that the gene contains introns

Supplementary Files

This is a list of supplementary files associated with this preprint. Click to download.

- Additionalfile.xlsx
- figureS1.doc
- AgarosegelelectrophoresisofPCRamplificationproductsoffouroverlappingregions.pdf